

# Improving the decoding performance of CA-polar codes

Jiewei Feng, Peihong Yuan, Ken R. Duffy and Muriel Médard

**Abstract**—We investigate the use of modern code-agnostic decoders to convert CA-SCL from an incomplete decoder to a complete one. When CA-SCL fails to identify a codeword that passes the CRC check, we apply a code-agnostic decoder that identifies a codeword that satisfies the CRC. We establish that this approach gives gains of up to 0.2 dB in block error rate for CA-Polar codes from the 5G New Radio standard. If, instead, the message had been encoded in a systematic CA-polar code, the gain improves to 0.2 ~ 1 dB. Leveraging recent developments in blockwise soft output, we additionally establish that it is possible to control the undetected error rate even when using the CRC for error correction.

**Index Terms**—CA-polar, SCL, GRAND, GCD, Soft Output

## I. INTRODUCTION

**P**OLAR codes were introduced by Arikan in 2008 and are capacity achieving for binary-input discrete memoryless channel (B-DMC) [1]. When concatenated with a cyclic redundancy check (CRC) as an outer code, the resulting CRC-Aided polar (CA-polar) codes were adopted in the 5G New Radio (NR) standard for all control channel communications [2]. CRC-Aided Successive Cancellation List (CA-SCL) decoding, e.g. [3], [4], is a prominent decoder for CA-polar codes. It operates by first providing a list of candidates using SCL decoding followed by performing CRC checks for each candidate. If no candidate passes the CRC check, a decoding failure is declared. A complete decoder always provides a codeword while an incomplete one does not [5]. As a result, CA-SCL is an incomplete decoder.

While the CRC in CA-polar codes is used for error detection, it can be more extensively leveraged for error correction using recent advances. Guessing Random Additive Noise Decoding (GRAND) [6]–[8] and Guessing Codeword Decoding (GCD) [9], [10] are code-agnostic and Maximum Likelihood (ML), or near ML, decoders that can efficiently decode a broad class of codes, including CRC codes. Those algorithms can be highly parallelized and many efficient circuits and chips have been published for GRAND variants, e.g. [11]–[16], which can be further accelerated by using techniques from [17]–[19]. In this paper, we investigate the application of one of these recent code-agnostic decoders as an outer decoder that uses the CRC code for error correction when CA-SCL fails. This results in a complete decoder that we call Complete CA-SCL (CCA-SCL).

Compared to the standard polar codes, systematic polar codes provide an advantage in terms of bit error rate (BER) while guaranteeing the same block error rate (BLER) [20].

This work was supported by the Defense Advanced Research Projects Agency (DARPA) under Grant HR00112120008

J. Feng and K. R. Duffy, Northeastern University, (e-mails: {feng.ji,k.duffy}@northeastern.edu).

P. Yuan and M. Médard, Massachusetts Institute of Technology, (e-mails: {phyuan, medard}@mit.edu).

The decoding process of systematic polar codes remains the same, except that the information bits are directly available in the encoded codeword. A systematic polar code concatenated with a CRC code results in a systematic CA-polar code. Our results demonstrate that additional improvement can be achieved using the proposed decoding scheme if a systematic CA-polar code is used.

One motivation for adopting CA-polar codes in 5G NR was to support Ultra-Reliable Low-Latency Communication (URLLC). Recently, Soft output (SO) variants of GRAND, GCD, and SCL have been introduced, which are known as SOGRAND [21], [22], SO-GCD [23] and SO-SCL [24], respectively. These variants can provide blockwise SO in the form of an accurate estimate of the likelihood that each proposed decoding in a list is correct. The key enhancement over earlier approaches, e.g. [25], is the development of a per-decoding estimate of the likelihood that the transmitted codeword is not in the decoded list, which removes the requirement of list decoding while enabling near-optimal SO compared to a exhaustively computed SO, [26]. In addition to using the outer decoder, we employ these SO algorithms to provide reliable SO for undetected error rate (UER) control, which facilitates the use of the CRC for error correction as well as detection. In particular, accurate SO for CA-SCL can be adapted from SO-SCL by leveraging the CRC outer code as detailed in Section III-B.

The remainder of this paper is organized as follows. Section II introduces the basic setups. Section III describes the CCA-SCL decoding pipeline, with simulation results given in Section IV. A conclusion is given in Section V.

## II. PRELIMINARIES

Consider a binary message denoted as  $\Phi^M = (\Phi_1, \dots, \Phi_M) \in \mathbb{F}_2^M$  where  $M$  is the number of information bits. The encoding process of a CA-polar code can be described as follows. The message  $\Phi^M$  is first encoded using an outer CRC code that is systematic, which is specified by the generator matrix  $G_O$  with dimension  $M$  by  $K$ , through  $\Phi^K = \Phi^M G_O$ .  $H_O$  denotes the parity check matrix of  $G_O$ . The sequence  $\Phi^K$  is then encoded using a polar code as the inner code, which is specified by the generator matrix  $G_I$  with dimension  $K$  by  $N$ , through  $X^N = (X_1, \dots, X_N) = \Phi^K G_I = \Phi^M G_O G_I$ .

The polar code specified by  $G_I$  can be equivalently described by the following: Let  $\mathcal{F} \subset \{1, \dots, N\}$  record the locations of the frozen bits in a sequence with length  $N = 2^n$  for some  $n$  and  $|\mathcal{F}| = N - K$ . We define  $\mathcal{A} = \{1, \dots, N\} \setminus \mathcal{F}$  where  $\setminus$  is the set minus operation. Denote  $G_{[K,N]}$  to be the  $K$  by  $N$  matrix such that the columns in the set  $\mathcal{F}$  form a  $K$  by  $N - K$  zero matrix and the rest of the columns form a

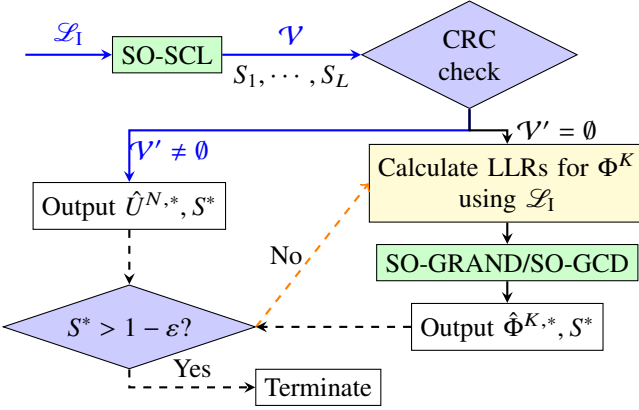


Fig. 1. Pipeline of the proposed CCA-SCL decoder. Blue lines represent CA-SCL. Dashed lines represent new additions.

$K$  by  $K$  identity matrix. The sequence  $\Phi^K$  is first expanded by  $U^N = \Phi^K G_{[K,N]}$ , where the subsequence  $U_{\mathcal{A}}$  records  $\Phi^K$  and the subsequence  $U_{\mathcal{F}}$  is a zero sequence. Let  $F^{\otimes n}$  denote the  $n$ -th Kronecker power of  $F$  and

$$F = \begin{bmatrix} 1 & 0 \\ 1 & 1 \end{bmatrix}.$$

Then the expanded sequence is encoded by  $F^{\otimes n}$ , resulting in  $\Phi^K G_1 = \Phi^K G_{[K,N]} F^{\otimes n}$ . Note that  $F^{\otimes n}$  is its own inverse.

After the encoding,  $X^N$  is transmitted via  $N$  independent uses of a B-DMC, and the receiver observes channel output  $Y^N \in \mathbb{R}^N$ . Given knowledge of the channel, the conditional pdf of  $Y$  given  $X$ ,  $f_{Y|X}$ , can be calculated. The LLR of the  $i$ -th received bit is denoted as

$$\mathcal{L}_{1,i} = \log \frac{f_{Y|X}(Y_i|X_i = 1)}{f_{Y|X}(Y_i|X_i = 0)}.$$

and we denote  $\mathcal{L}_1 = (\mathcal{L}_{1,1}, \dots, \mathcal{L}_{1,N})$ , where  $1$  is used to indicate that the LLR is related to the  $N$  bits resulting from encoding through the inner code.

A SCL decoder [4] decodes and provides a list of  $L$  candidates  $\hat{U}^{N,1}, \hat{U}^{N,2}, \dots, \hat{U}^{N,L}$  for  $U^N$ . Let  $\mathcal{V}$  denote the set of candidates. A LLR-based SCL decoder provides a path metric (PM) [27] for each of the candidates to indicate which candidate is more reliable. For each candidate  $\hat{U}^{N,i}$ , SO-SCL [24] provides a corresponding SO,  $S_i \in [0, 1]$ , which serves as a probability estimate for whether the candidate is correct, i.e., whether  $\hat{U}^{N,i} = U^N$ . Note that the rank order of the PM for each candidate is the same as the rank order of the SO for each candidate. Let  $\mathbf{0}$  denote the zero vector. Each candidate in  $\mathcal{V}$  is examined by the CRC check. Denote  $\mathcal{V}' = \{\hat{U}^{N,i} \mid \hat{U}^{N,i} \in \mathcal{V}, H_0(\hat{U}^{N,i})^T = \mathbf{0}\}$  to be the subset of  $\mathcal{V}$  such that  $\mathcal{V}'$  contains all the candidates that pass the CRC check. Let  $S^* = \max\{S_i \mid \hat{U}^{N,i} \in \mathcal{V}'\}$  denote the maximum SO within the remaining candidates and the corresponding candidate  $\hat{U}^{N,*} \in \{\hat{U}^{N,i} \mid S_i = S^*\} \subseteq \mathcal{V}'$  will be the decoded message. If  $\mathcal{V}' = \emptyset$ , a decoding failure is declared.

### III. PROPOSED PIPELINE FOR CCA-SCL

Here we investigate a decoding scheme based on CA-SCL to improve BLER with accurately controllable UER, which

is illustrated in Fig. 1. SO-SCL first decodes as explained in Section II. When  $\mathcal{V}' \neq \emptyset$ , the most reliable candidate is selected. These operations are similar to a traditional CA-SCL decoder except that SCL is replaced by SO-SCL in order to provide accurate SO for UER control. In Fig. 1, the processes for standard CA-SCL decoding are indicated in blue.

When  $\mathcal{V}' = \emptyset$ , CA-SCL declares a failure. Instead, we apply a decoder for the outer code by using the LLRs corresponding to  $\Phi^K = U_{\mathcal{A}}$  and  $H_0$ , which will be described in detail in Section III-A. The decoder for the outer code is called the *outer decoder*, and possible choices of the outer decoder includes SO-GCD [23] and SOGRAND [22]. The procedure of applying the outer decoder is demonstrated on the right side of Fig. 1. The outer decoder provides a decoded candidate  $\hat{\Phi}^{K,*}$  with corresponding SO  $S^*$ . The proposed pipeline, regardless of whether  $\mathcal{V}'$  is empty, always provides a valid codeword  $\hat{U}^{N,*}$  or  $\hat{\Phi}^{K,*}$  with its SO  $S^*$ , which enables additional operations that are highlighted by dashed arrows in Fig. 1.

One new possibility is to perform a threshold test of the SO for UER control, as highlighted in black dashed lines. By adjusting the threshold  $\epsilon$ , it is possible to control the tradeoff between BLER and UER. For accurate SO, the tradeoff is optimum in the sense that there is no other decision rule that can have lower BLER and UER simultaneously as established in [25]. A second possibility is to activate the outer decoder whenever the decoded codeword from CA-SCL fails the threshold test, which is highlighted in the orange dashed line.

#### A. Decoding using outer decoder

When CA-SCL fails to decode, we apply an outer decoder to estimate  $\Phi^K$  with the following inputs: LLRs corresponding to  $\Phi^K = U_{\mathcal{A}}$  called *outer LLR* and the CRC parity check matrix  $H_0$ . However, the outer LLR can not be directly observed from  $\mathcal{L}_1$  since the polar code is not systematic, leading to the following calculation. Conditioned on the channel LLR, the likelihood that  $X_i = 1$ , denoted as  $B_{1,i}$ , can be calculated as

$$B_{1,i} = P(X_i = 1 \mid \mathcal{L}_1) = \frac{1}{1 + e^{-\mathcal{L}_{1,i}}}. \quad (1)$$

Let  $\pi(i)$  denote the position in  $U^N = \Phi^K G_{[K,N]}$  that records the value of  $\Phi_i$ . Let  $F_{i,j}^{\otimes n}$  denote the entry of  $F^{\otimes n}$  at the  $i$ -th row and the  $j$ -th column. Since  $\Phi^K G_{[K,N]} F^{\otimes n} = \Phi^K G_1 = X^N$ ,  $\Phi^K G_{[K,N]} = U^N = X^N F^{\otimes n}$ . Hence the likelihood that  $\Phi_i = 1$  conditioned on the channel LLR can be calculated using Lemma 1 of [28], i.e.,

$$B_{0,i} = P(\Phi_i = 1 \mid \mathcal{L}_1) = \frac{1}{2} - \frac{1}{2} \prod_{j=1}^N \left( 1 - 2B_{1,j} F_{j,\pi(i)}^{\otimes n} \right), \quad (2)$$

which can be converted to outer LLR  $\mathcal{L}_{0,i}$  for the  $K$  bits in  $\Phi^K$  analogously to eq. (1). This calculation leads to two consequences that impact the performance of the outer decoder, which are presented in Lemmas 1 and 2.

**Lemma 1.** Let  $|\mathcal{L}_{1,j}|$  denote the reliability of the hard decision for  $X_j$  based on  $\mathcal{L}_{1,j}$ . Similarly, let  $|\mathcal{L}_{0,i}|$  denote the reliability of the hard decision for  $\Phi_i$  based on  $\mathcal{L}_{0,i}$ . Denote

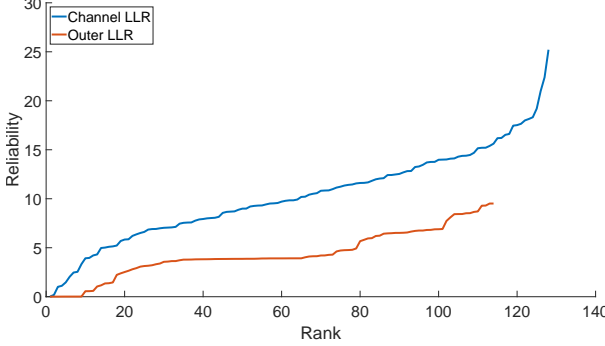


Fig. 2. Example comparison between channel LLR  $\mathcal{L}_{I,i}$  and outer LLR  $\mathcal{L}_{O,j}$ . Code parameters are  $[N, K, M] = [128, 114, 90]$  and  $E_b/N_0 = 6$  dB. The blue line represents the reliabilities  $|\mathcal{L}_{I,i}|$  for  $i = 1, \dots, N$  where the reliabilities are ordered from the least to the highest. The orange line represents the ordered reliabilities  $|\mathcal{L}_{O,j}|$  for  $j = 1, \dots, K$ . As depicted by the figure, converting the LLRs through eq. (2) results in less reliability.

$X_i = \{s | F_{s, \pi(i)}^{\otimes n} = 1\}$  so that  $\Phi_i = \bigoplus_{s \in X_i} Y_s$  where  $\bigoplus$  denotes the summation in  $\mathbb{F}_2$ .  $X_i$  represents the set of bits in  $X^N$  that can be used to recover  $\Phi_i$ . Then  $|\mathcal{L}_{O,i}| \leq |\mathcal{L}_{I,i}|$  for all  $i, j$  such that  $j \in X_i$ .

*Proof.* By eq. (1),  $|1/2 - B_{I,i}| = (e^{|\mathcal{L}_{I,i}|} - 1)/(2e^{|\mathcal{L}_{I,i}|} + 2)$ , which implies that  $|1/2 - B_{I,i}|$  is a monotone increasing function of the reliability for the corresponding bit. A parallel statement holds for  $|1/2 - B_{O,i}|$ . Hence it suffices to show  $|1/2 - B_{O,i}| \leq |1/2 - B_{I,j}|$  for all  $i, j$  such that  $j \in X_i$ :

$$\left| \frac{1}{2} - B_{O,i} \right| = 2^{|X_i|-1} \prod_{j \in X_i} \left| \frac{1}{2} - B_{I,j} \right| \leq \left| \frac{1}{2} - B_{I,j} \right|$$

for all  $j$  such that  $j \in X_i$ .  $\square$

Lemma 1 implies that  $\mathcal{L}_{O,i}$  converted from  $\mathcal{L}_I$  is generally less reliable than  $\mathcal{L}_{I,j}$  that is used to calculate  $\mathcal{L}_{O,i}$ . The inequality is strict if  $U_i$  corresponds to multiple bits in  $X^N$  through eq. (2). Fig. 2 illustrates this difference of reliabilities.

**Lemma 2.** For any pair of  $(i, j)$ , let  $X_{i,j} = X_i \cap X_j$ . Define  $p_{i \setminus j} := \frac{1}{2} - \frac{1}{2} \prod_{s \in X_i \setminus X_{i,j}} (1 - 2B_{I,s})$  and  $p_{i \setminus j} := 0$  if  $X_i \subseteq X_j$ . Define  $p_{i,j} := \frac{1}{2} - \frac{1}{2} \prod_{s \in X_{i,j}} (1 - 2B_{I,s})$  and  $p_{i,j} := 0$  if  $X_{i,j} = \emptyset$ . Then the covariance  $\text{Cov}(\Phi_i, \Phi_j | \mathcal{L}_I) = 0$  if and only if one of the following holds: 1)  $p_{i,j} \in \{0, 1\}$ ; or 2)  $p_{i \setminus j} = \frac{1}{2}$  or  $p_{j \setminus i} = \frac{1}{2}$ .

*Proof.* We will omit the notation for conditioning on  $\mathcal{L}_I$  throughout the proof as all calculations will be done with the conditioning. Given a pair  $i$  and  $j$ , notice that  $\Phi_i = \left( \bigoplus_{s \in X_i \setminus X_{i,j}} X_s \right) \oplus \left( \bigoplus_{s \in X_{i,j}} X_s \right)$  and similarly for  $\Phi_j$ . Let  $\bigoplus_{s \in X} X_s = 0$  if  $X = \emptyset$ . The same approach as in eq. (2) leads to  $P\left(\bigoplus_{s \in X_{i,j}} X_s = 1\right) = p_{i,j}$ ,  $P\left(\bigoplus_{s \in X_i \setminus X_{i,j}} X_s = 1\right) = p_{i \setminus j}$ , and  $P\left(\bigoplus_{s \in X_j \setminus X_{i,j}} X_s = 1\right) = p_{j \setminus i}$ . The covariance can then be calculated directly, yielding  $\text{Cov}(\Phi_i, \Phi_j) = p_{i,j}(1 - p_{i,j})(1 - 2p_{i \setminus j} - 2p_{j \setminus i} + 4p_{i \setminus j}p_{j \setminus i})$ .  $\square$

Condition 1) is satisfied when the demodulated bits with indices in  $X_{i,j}$  have infinite reliability or  $\Phi_i, \Phi_j$  are affected by disjoint sets of  $X^N$  so that  $X_{i,j} = \emptyset$ . However, in polar coding,

$X_{i,j} \neq \emptyset$  by the construction of  $F^{\otimes n}$ . Therefore, condition 1) happens with probability zero. Condition 2) is satisfied when all the bits with indexes in  $X_{i \setminus j} \cup X_{j \setminus i}$  have reliabilities equal to zero, which has probability zero. Therefore, after converting the channel LLRs to LLRs corresponding to  $\Phi^K$ , the converted LLRs are correlated, resulting in degradation if the outer decoder assumes  $\Phi_i, \Phi_j$  are independent for all  $i, j$ .

While simulation results will be given in Section IV, Lemmas 1 and 2 indicate that it is possible to achieve higher performance if the two issues can be resolved. In this paper, we demonstrate that systematic polar code [20] can be used to avoid both issues. The encoding process of a systematic polar code can be done by methods described in [29], [30], which enables the outer LLR to be directly observed from the channel LLR. Instead of recording the message  $\Phi^K$  in  $U_{\mathcal{A}}$ , let  $X_{\mathcal{A}}$  record  $\Phi^K$ . The usual polar encoding is performed for the first time to get  $U^N = X_{\mathcal{A}}G_1$ . Then only the part  $U_{\mathcal{A}}$  is encoded for the second time by  $X^N = U_{\mathcal{A}}G_1$ . The resulting  $X_{\mathcal{A}}$  maintains the record of  $\Phi^K$  with  $X_{\mathcal{F}}$  representing the redundant bits. A SCL decoder can decode with the same procedure as decoding non-systematic polar codes except that the information bits are now recorded in  $X_{\mathcal{A}}$  instead of  $U_{\mathcal{A}}$ . Applying systematic polar code in CA-polar, the CRC-encoded message is then recorded in  $X_{\mathcal{A}} = \Phi^K$  instead, whose corresponding LLRs can be directly observed from  $\{\mathcal{L}_{I,i} | i \in \mathcal{A}\}$ , avoiding the degradation caused by conversion. Simulation results in Section IV demonstrate the improvement extracted using systematic CA-polar codes.

### B. Managing UER with SO-SCL adapted to CA-polar

When a decoded message is provided with a blockwise SO  $S^*$ , the decoding can be tagged for erasure if  $S^* < 1 - \epsilon$ . This threshold test can be used to control UER with the targeted UER  $\epsilon$ . In CCA-SCL, the outer decoder SOGRAND or SO-GCD is used to provide blockwise SO for error detection through the threshold test. In this section, we will adapt the SO-SCL calculation to CA-SCL so that all decoded codewords produced in the pipeline are paired with a blockwise SO, which can be used to control UER.

We first give an overview of SO-SCL [22] for polar-like codes. We denote  $U^i$  to be the subsequence of  $U^N$  such that  $U^i = (U_1, \dots, U_i)$ . Assume the observed channel output is  $Y^N = y^N$ . Let  $Q_{U^N | Y^N}$  denote an auxiliary conditional probability mass function (PMF) as described in [24]. The SC decoding performs a greedy search and identifies a sequence  $\hat{u}^N$  such that  $\hat{u}_{\mathcal{F}}^N = \mathbf{0}$ . For SCL, up to  $L$  paths are explored in parallel, resulting in  $L$  candidates as output which are recorded in  $\mathcal{V}$ . The decoding process can be represented by a tree search with depth  $N$ . Each path with length  $N$  in the tree represents a sequence  $\hat{u}^N \in \mathbb{F}_2^N$ . SCL keeps a record of  $L$  paths that satisfy the frozen constraints, hence dividing the tree into three parts:

- Visited paths* denote the  $L$  paths provided by SCL, where all of them satisfy the frozen constraints.
- Unvisited valid paths* are the paths that satisfy the frozen constraints but have not been fully explored due to memory and complexity issues.
- Invalid paths* are the paths that do not meet the frozen constraints, where a path  $\hat{u}^N \in \mathbb{F}_2^N$  is invalid if  $\hat{u}_{\mathcal{F}}^N \neq \mathbf{0}$ .

In this paper, the term *valid* refers to whether the path satisfies the frozen constraints without considering the CRC. Recall that  $\mathcal{V}$  is the set of  $L$  visited paths. We denote  $\mathcal{W}$  to be the set of all unvisited valid paths. The optimal blockwise SO for polar-like codes with the knowledge of all possible codewords is given by  $\Gamma(y^N, \hat{u}^N) =$

$$\frac{Q_{U^N|Y^N}(\hat{u}^N|y^N)}{\sum_{u^N \in \mathcal{V}} Q_{U^N|Y^N}(u^N|y^N) + \sum_{u^N \in \mathcal{W}} Q_{U^N|Y^N}(u^N|y^N)}. \quad (3)$$

The numerator in (3) represents the likelihood of a decoded sequence  $\hat{u}^N$  while the denominator represents the sum of likelihoods of all possible decoding paths satisfying the frozen constraints. The denominator is called the codebook probability. Forney's approximation [25] to equation (3) is given by

$$\frac{Q_{U^N|Y^N}(\hat{u}^N|y^N)}{\sum_{u^N \in \mathcal{V}} Q_{U^N|Y^N}(u^N|y^N)}, \quad (4)$$

where the second summation in the denominator of (3) is omitted, i.e., the SO is calculated conditioned on the transmitted codeword being in the list of visited paths. Note that the assumption requires that the list size is at least two.

In contrast, [24] considers the omitted term in (4), which represents the likelihood of unvisited valid paths. The omitted term  $\sum_{u^N \in \mathcal{W}} Q_{U^N|Y^N}(u^N|y^N)$  is approximated by a quantity  $Q_{\mathcal{W}}^*$  which can be readily calculated through the decoding process (see [24] for details). This leads to the approximation for (3) as

$$\Gamma(y^N, \hat{u}^N) \approx \Gamma^*(y^N, \hat{u}^N) = \frac{Q_{U^N|Y^N}(\hat{u}^N|y^N)}{\sum_{u^N \in \mathcal{V}} Q_{U^N|Y^N}(u^N|y^N) + Q_{\mathcal{W}}^*}. \quad (5)$$

It is verified in [24] that the blockwise SO using equation (5) is accurate and outperforms Forney's approximation for polar-like codes. Note that each  $\hat{U}^N$  corresponds to a unique sequence of  $\hat{X}^N$ . This ensures that the same SO calculation can be applied in systematic polar codes.

For CA-polar codes, we can leverage the outer code to improve the accuracy of SO-SCL since not all the valid decoding paths in SCL can pass the CRC check. For any valid decoding path that violates the CRC check, its likelihood of being the transmitted codeword is zero. Recall that  $\mathcal{V}' \subseteq \mathcal{V}$  denotes the set of visited paths that pass the CRC check. The summation  $\sum_{u^N \in \mathcal{V}}$  in (5) is hence replaced by  $\sum_{u^N \in \mathcal{V}'}$ .

Recall that the length of the CRC is  $K - M$ , and  $\mathcal{W}$  denotes the set of unvisited valid paths, which covers the  $2^K - L$  paths satisfying the frozen constraints. Note that  $Q_{\mathcal{W}}^*$  approximates the sum of likelihood of the  $2^K - L$  unvisited valid paths regardless of the CRC check. Within the unvisited valid paths, around  $[2^M - L, 2^M]$  out of  $2^K - L$  of them are valid codewords that can pass the CRC check. By assuming that the unvisited valid paths satisfying the CRC check are uniformly distributed within all unvisited valid paths,  $2^{M-K}Q_{\mathcal{W}}^*$  can be used to approximate the sum of the likelihood of the unvisited valid paths that can pass the CRC check. Combining the two modifications yields (6), which provides the blockwise SO calculation for CA-polar codes using SO-SCL.

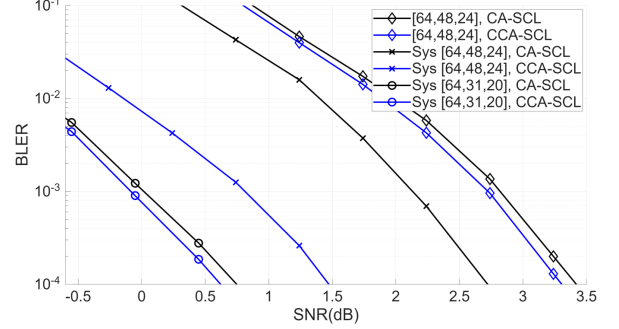


Fig. 3. BLER performance of CA-SCL and Complete CA-SCL (CCSCL) with BPSK subject to AWGN.

$$\Gamma^*(y^N, \hat{u}^N) = \frac{Q_{U^N|Y^N}(\hat{u}^N|y^N)}{\sum_{u^N \in \mathcal{V}'} Q_{U^N|Y^N}(u^N|y^N) + 2^{M-K}Q_{\mathcal{W}}^*}. \quad (6)$$

Note that equation (6) only considers the length of the outer code  $K - M$  and hence is compatible with any concatenated polar codes. More generally, for a concatenated code with outer code represented as a map  $G_1 : \mathbb{F}_2^M \rightarrow \mathbb{F}_2^K$  and an inner code represented as a map  $G_2 : \mathbb{F}_2^K \rightarrow \mathbb{F}_2^N$ , where the outer code serves as an error detection code only and a decoder for the inner code is able to produce the blockwise SO using similar ideas from [22]–[24], similar modification can be conducted to incorporate the outer code for SO calculation.

#### IV. SIMULATIONS

For simulation, we use BPSK and AWGN. The CRC parameters are chosen from the 5G NR standard. Fig. 3 demonstrates the BLER improvement for CCA-SCL without the threshold test. Black lines represent CA-SCL while blue lines represent CCA-SCL with SOGRAND as the outer decoder with list size one. SO-GCD and SOGRAND have similar performance and hence we only present the results with SO-GCD driven by ORBGRAND [8]. Lines with diamonds represent using non-systematic CA-polar code with dimension  $[N, K, M] = [64, 48, 24]$  where the SCL decoder has list size  $L = 4$  and the outer decoder is able to find a correct codeword around 50% of the time when CA-SCL fails. Lines with crosses represent using systematic CA-polar code with dimension  $[64, 48, 24]$  where the SCL decoder has list size  $L = 16$  and the outer decoder is able to find a correct codeword around 99% of the time when CA-SCL fails. Lines with circles represent using systematic CA-polar code with dimension  $[64, 31, 20]$  where the SCL decoder has list size  $L = 4$  and the outer decoder successfully identifies the correct codeword around 40% of the time. As depicted in Fig. 3, CCA-SCL provides around 0.2 dB improvement for non-systematic CA-polar codes and up to 1 dB gain for systematic CA-polar codes.

Fig. 4 provides verification of (6) for CA-SCL and demonstrates the effectiveness of using SO for UER control in the pipeline. For verification of (6), we use CA-SCL with a list size of eight to decode the  $[64, 43, 32]$  CA-polar code at  $E_b/N_0 = 2$  dB. Simulations are grouped based on the

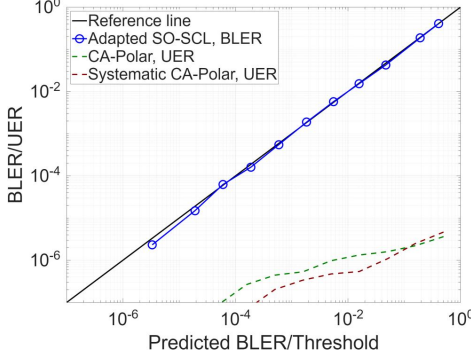


Fig. 4. Verification of SO calibration for a [64, 43, 32] CA-polar code.

predicted BLER  $1 - \Gamma^*(y^N, \hat{u}^N)$  within the intervals with endpoints  $10^0, 10^{-0.5}, 10^{-1}, \dots, 10^{-5}$ , where  $\Gamma^*$  is calculated using (6). For each group of simulations within an interval, the BLER is plotted against the average value of  $1 - \Gamma^*$ . The black line represents the function  $y = x$  as a reference. A plot similar to the black line indicates that the SO is accurate. The solid blue line represents (6) and demonstrates its accuracy. Note that (4) can also be adapted to CA-SCL by replacing  $\mathcal{V}$  with  $\mathcal{V}'$  in the summation of (4). However, this modification cannot provide a meaningful SO when  $|\mathcal{V}'| = 1$  because the decoded list size is one. In contrast, if (4) is used directly, it provides an underestimated SO because it includes the sequence that violates the CRC check in the denominator.

For verification of UER control, we employ the pipeline described in Fig. 1. Using the same code dimension and list size as above, we employ SO-GCD as the outer decoder and simulate at  $E_b/N_0 = 5$  dB. UER versus the threshold  $\epsilon$  is plotted, with the black line serving as a reference line. The dashed red line represents the simulation for non-systematic CA-polar while the dashed green line represents systematic CA-polar. Both lines are lower than the reference line, which implies that CCA-SCL can maintain UER control within the targeted threshold.

## V. CONCLUSION

In this paper, we investigate a decoding pipeline based on CA-SCL with additional decoding step using an outer decoder that makes for a complete decoder. By leveraging the recently developed SO formulae that consider likelihood of unvisited codewords, the pipeline can also provide blockwise SO for UER control. Simulations show that CCA-SCL has around 0.2 dB gain in BLER when using CA-polar code under 5G NR standard. In addition, the same decoder can lead to 0.2 ~ 1 dB gain when the CA-polar code is encoded in systematic format.

## REFERENCES

- [1] E. Arikan, “Channel polarization: A method for constructing capacity-achieving codes for symmetric binary-input memoryless channels,” *IEEE Trans. Inf. Theory*, vol. 55, no. 7, pp. 3051–3073, 2009.
- [2] V. Bioglio, C. Condo, and I. Land, “Design of polar codes in 5G new radio,” *IEEE Commun. Surv. Tut.*, vol. 23, no. 1, pp. 29–40, 2021.
- [3] K. Niu and K. Chen, “CRC-aided decoding of polar codes,” *IEEE Commun. Lett.*, vol. 16, no. 10, pp. 1668–1671, 2012.
- [4] I. Tal and A. Vardy, “List decoding of polar codes,” *IEEE Trans. Inf. Theory*, vol. 61, no. 5, pp. 2213–2226, 2015.
- [5] R. E. Blahut, *Algebraic codes for data transmission*. Cambridge university press, 2003.
- [6] K. R. Duffy, J. Li, and M. Médard, “Capacity-achieving guessing random additive noise decoding (GRAND),” *IEEE Trans. Inf. Theory*, vol. 65, no. 7, pp. 4023–4040, 2019.
- [7] A. Solomon, K. R. Duffy, and M. Médard, “Soft maximum likelihood decoding using GRAND,” in *IEEE ICC*, 2020.
- [8] K. R. Duffy, W. An, and M. Medard, “Ordered reliability bits guessing random additive noise decoding,” *IEEE Trans. Signal Proc.*, vol. 70, pp. 4528 – 4542, 2022.
- [9] X. Ma, “Guessing what, noise or codeword?” *IEEE ITW*, 2024.
- [10] X. Zheng and X. Ma, “A universal list decoding algorithm with application to decoding of polar codes,” *IEEE Trans. Inf. Theory*, vol. 71, no. 2, pp. 975–995, 2025.
- [11] S. M. Abbas, T. Tonnelier, F. Ercan, M. Jalaleddine, and W. J. Gross, “High-throughput VLSI architecture for soft-decision decoding with ORBGRAND,” in *IEEE Int. Conf. Acoust. Speech and Signal Process.*, 2021, pp. 8288–8292.
- [12] C. Condo, “A fixed latency ORBGRAND decoder architecture with LUT-aided error-pattern scheduling,” *IEEE Trans. Circuits Sys. I: Regular Papers*, vol. 69, no. 5, pp. 2203–2211, 2022.
- [13] L. D. Blanc, V. Herrmann, Y. Ren, C. Müller, A. T. Kristensen, A. Levisse, Y. Shen, and A. Burg, “A GRANDAB decoder with 8.48 Gbps worst-case throughput in 65nm CMOS,” in *IEEE ESSERC*, 2024, pp. 685–688.
- [14] A. Riaz, A. Yasar, F. Ercan, W. An, J. Ngo, K. Galligan, M. Médard, K. R. Duffy, and R. T. Yazicigil, “A sub-0.8-pJ/bit universal soft-detection decoder using ORBGRAND,” *IEEE J. Solid-State Circuits*, vol. 60, no. 7, pp. 2645–2659, 2025.
- [15] S. M. Abbas, M. Jalaleddine, C.-Y. Tsui, and W. J. Gross, “Improved Step-GRAND: low-latency soft-input guessing random additive noise decoding,” *IEEE Trans. Very Large Scale Integr. (VLSI) Syst.*, vol. 33, no. 4, pp. 1028–1041, 2025.
- [16] E. Kizilates, A. Riaz, A. Bali, M. Grunde, M. Médard, K. R. Duffy, and R. T. Yazicigil, “Low-latency modulation- and correlation-adaptive ORBGRAND-AI decoder,” in *IEEE ESSERC*, 2025.
- [17] M. Rowshan and J. Yuan, “Constrained error pattern generation for GRAND,” in *IEEE Int. Symp. on Inf. Theory*, 2022.
- [18] —, “Segmented GRAND: Complexity reduction through sub-pattern combination,” *IEEE Trans. Commun.*, vol. 73, no. 8, pp. 5607–5620, 2025.
- [19] L. Rapp, J. Feng, M. Médard, and K. R. Duffy, “A balanced tree transformation to reduce GRAND queries,” in *IEEE ISIT*, 2025.
- [20] E. Arikan, “Systematic polar coding,” *IEEE Commun. Lett.*, vol. 15, no. 8, pp. 860–862, 2011.
- [21] K. Galligan, P. Yuan, M. Médard, and K. R. Duffy, “Upgrade error detection to prediction with GRAND,” in *IEEE Glob. Commun. Conf.*, 2023, pp. 1818–1823.
- [22] P. Yuan, M. Medard, K. Galligan, and K. R. Duffy, “Soft-output (SO) GRAND and iterative decoding to outperform LDPC codes,” *IEEE Trans. Wireless Commun.*, pp. 1–1, 2025.
- [23] K. R. Duffy, P. Yuan, J. Griffin, and M. Médard, “Soft-output guessing codeword decoding,” *IEEE Commun. Lett.*, vol. 29, no. 2, pp. 328–332, 2025.
- [24] P. Yuan, K. R. Duffy, and M. Médard, “Soft-output successive cancellation list decoding,” *IEEE Trans. Inf. Theory*, vol. 71, no. 2, pp. 1007–1017, 2025.
- [25] G. Forney, “Exponential error bounds for erasure, list, and decision feedback schemes,” *IEEE Trans. Inf. Theory*, vol. 14, no. 2, pp. 206–220, 1968.
- [26] J. Feng, K. R. Duffy, and M. Médard, “Leveraging code structure to improve soft output for GRAND, GCD, OSD, and SCL,” *arXiv:2503.16677*, 2025.
- [27] A. Balatsoukas-Stimming, M. B. Parizi, and A. Burg, “LLR-based successive cancellation list decoding of Polar codes,” *IEEE Trans. Signal Process.*, vol. 63, no. 19, pp. 5165–5179, 2015.
- [28] R. Gallager, “Low-density parity-check codes,” *IRE Trans. Inf. Theory*, vol. 8, no. 1, pp. 21–28, 1962.
- [29] G. Sarkis, I. Tal, P. Giard, A. Vardy, C. Thibeault, and W. J. Gross, “Flexible and low-complexity encoding and decoding of systematic polar codes,” *IEEE Trans. Commun.*, vol. 64, no. 7, pp. 2732–2745, 2016.
- [30] G. Sarkis, P. Giard, A. Vardy, C. Thibeault, and W. J. Gross, “Fast polar decoders: Algorithm and implementation,” *IEEE J. Sel. Areas Commun.*, vol. 32, no. 5, pp. 946–957, 2014.